

Detection of Two Phases Coexisting at the Phase Transition Temperature in LiNbO₃ Single Crystal by using Raman Spectroscopy

Rasha M. Khafagy

*Physics Department, Girls College for Arts, Science and Education,
Ain Shams University, Cairo, Egypt*

Low temperature Raman spectroscopic study has been performed on a Z-cut LiNbO₃ single crystal in the case of Z(xy)Z configuration. Low temperature studies were performed to be far from the critical temperature, which is known to be at 1165°C in Lithium Niobate, looking for possible anomalies or precursors of the phase transition. Room temperature Raman spectra revealed the presence of the E[TO] modes only, as predicted by the Raman selection rules and group theory for the Z(xy)Z configuration. Comparison of the Raman spectra at room temperature and lower temperatures shows a strong intensity attenuation and progressive reduction in the intensity of the Raman peaks, in addition to the appearance of the A1[TO] modes at 279, 336 and 629 cm⁻¹, which are known to be forbidden modes of the Z(xy)Z configuration. A1[TO] modes resulted from the splitting of 581, 332 and 269 cm⁻¹ vibrational modes into two branches below -100°C. Since the original 581 cm⁻¹ band corresponds to a totally symmetric NbO₆ stretching mode, this splitting was interpreted as due to a distortion in the NbO₆ structure leading to two distinct sites for the NbO₆ unit. This effect is explained as a result of inharmonic vibrations (quasi-soft-mode) and the two-phonon state. The temperature dependence of the band parameters showed an inversion point at -100°C, and discontinuity near +150°C. These results indicate that a phase transition occurs at -100°C on cooling and near +150°C on heating, indicating that an abnormality in the structure of LiNbO₃ is taking place.

1. Introduction:

Lithium Niobate (LN) is a key material for photonics, both for basic research and industrial applications [1]. Its electro-, acousto- and nonlinear-optical properties allow the realization of active and passive integrated optical devices. However, an inherent problem with guided-wave devices in LN is their quite low resistance to photorefractive (PR) damage [2 and 3]. At room temperature LN is a ferroelectric material, characterized with its high

electrooptic, piezoelectric and non-linear coefficients, together with high optical damage threshold and large birefringence which allows phase matching in addition to a broad spectral region of transparency (0.4-5 μm). These properties are very attractive for the integrated optics devices properties, and accordingly, serious attention has been paid to the preparation of high quality optical waveguides in this crystal [4].

It is known that the electrooptic coefficients and the non-linear properties of LN are correlated with the low frequency Raman vibrational modes [5] and, thus, the Raman spectra can provide valuable information. The assignment of the Raman spectra of pure LiNbO_3 has been studied by several authors [6-8] and directional dispersion of all first-order branches was studied, enabling the specialists to review the experiment and to correct the assignments [6]. The temperature dependence of the Raman and infrared spectra has been investigated, the attention being paid mostly to the presence of soft mode and to the high temperature ferroelectric–paraelectric phase transition [9-14]. These studies included a symmetry group analysis of the material below and above the critical temperature at 1165°C and soft mode behavior, where Infrared and Raman spectra were recorded mostly at high temperatures close to T_c . However, the nature of the observed spectral peculiarities, especially those in the low-frequency range, is still controversial. In this study Raman spectra were measured at lower temperatures far from the critical temperature looking for possible anomalies or precursors of the phase transition. Soft phonons were found in Raman spectra, as well as anomalies of the Raman scattering tensor at -100°C and $+150^\circ\text{C}$. These results could contribute to a better understanding of the vibrational structure of LiNbO_3 single crystals and suggest possible new applications. Also, appearance of new lines in addition to strong intensity attenuation has been detected in the Raman spectra of LiNbO_3 due to the reported here thermal treatment.

2. Experimental:

The used here single crystal was cut from a cylindrical one prepared using the zone refining technique in the form of a disc having 2 mm thick and 10 mm diameter. The Raman spectra was measured in back-scattering geometry at different temperatures using a BRUKER FT-Raman spectrometer of type RFS 100/S attached to BRUKER-IFS 66/S spectrometer equipped with Specac variable temperature cell (P/N 21525) originally designed for IR and Raman spectroscopic studies. The variable temperature cell is controlled via a temperature controller measuring in the range from -196°C to $+250^\circ\text{C}$ with the accuracy of $\pm 1^\circ\text{C}$. Nd:Yag laser operating at 1064 nm and highly sensitive liquid nitrogen cooled germanium detector were used.

3. Results and Discussion:

It is well known that the lattice of LiNbO_3 (Fig. (1)) is built of NbO_6 and LiO_6 octahedra, each Oxygen atom being shared between two Niobium and two lithium octahedral (Scheme1) [15]. The crystal structure of LN has $Rc3$ space group symmetry and $4A_1+9E$ Raman active modes as predicted by factor group analysis [16]. The vibrational modes of the LN crystals can be classified as internal modes of the NbO_6 octahedron, and the lattice transitions involving motion of the cations. Borstel and Merte [17] have calculated the frequencies of these 13 branches, and the predicted modes were found to depend on the relative orientation of the crystal with respect to the propagation axis and the polarization of the incident and scattered light [17]. Thus from Raman selection rules, only $E[\text{TO}]$ modes are expected in the $Z(xy)Z$ configuration, while one does expect to observe $A_1[\text{LO}] + E[\text{TO}]$ modes in the $Z(yy)Z$ case [17].

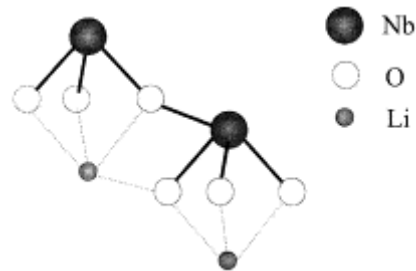


Figure (1): Lattice of LiNbO_3 .

Let us consider the z-cut sample in the case for $Z(xy)Z$ configuration, the room temperature Raman spectrum for $Z(xy)Z$ configuration shows the $E[\text{TO}]$ modes as predicted by the group theory. In order to account for any changes in the structure of this crystal that may occur before changing from the ferroelectric phase having the rhombohedra structure at room temperature, the Raman spectra were monitored in a temperature range from -196°C to $+225^\circ\text{C}$, taking into consideration that LiNbO_3 remains in the same state until 1250°C , at this point it becomes cubic [18]. Low temperature studies were performed to be far from the critical temperature, which is known to be at 1165°C in Lithium Niobate, looking for possible anomalies or precursors of the phase transition. Fig.1 shows the Raman shifts obtained for the LiNbO_3 crystal at five different temperatures, while Table (1) includes the experimentally obtained Raman modes of LiNbO_3 in addition to the corresponding symmetry and type of vibrations.

As a first approach, the comparison of the Raman spectra at room temperature and lower temperatures shows a progressive reduction in the intensity of the peaks. The intensity of a Raman scattering mainly depends on incident light intensity, the spectrometer characteristics, the concentration of atoms and their electronic polarizability, and other factors related to the environment (temperature, pressure, . . .) of the compound under study [19]. The absence of the 120 cm^{-1} peak can be used as an experimental criterion of structural perfection of LiNbO_3 crystals. The band at 120 cm^{-1} appears in the spectrum when there is a deviation from stoichiometric perfection [20]. The peak at 581 cm^{-1} represents an inharmonic two-phonon mode (totally symmetric NbO_6 stretching mode) as it was previously proposed [10, 21-23].

Table (1): Experimental peak positions, symmetry and type of Raman-active modes in LiNbO_3 single crystal at different temperatures

Experimental Raman active modes			Symmetry	Type of vibration
Low temp.	Room temp.	High temp.		
152.7	152.9	150.8	E	mutual nearly ip rocking of NbO_6 octahedra and nearly ip Li-vibrations (transitional motion of Li^+ cation with the internal octahedron NbO_6)
-----	187.3 (sh)	-----		
237.6	237.1	236.3	E	Nb-O bond rocking, Nb-O-Nb bending and ip Li-vibrations
261.5 (s)	-----	262.5 (vs)	E	ip Li-vibrations, weak Nb-O bond rocking
279.6 (s)	-----	-----	A_1	ip twisting of NbO_6 octahedra and op Li-vibrations
298.9 (sh)	-----	-----		
322.8 (s)	320 (sh)	325.4 (s)	E	O-Nb-O and Nb-O-Nb bending
337.3	-----	-----	A_1	sym O-Nb-O bending
371.7 (s)	365.7 (s)	359.2 (sh)	E	
432.6	432.2	430.8	E	O-Nb-O bending
581.7	581.2	577.6	E	totally symmetric NbO_6 stretching mode
629.4 (s)	-----	-----	A_1	sym Nb-O stretching
-----	660.5 (w)	-----	E	
-----	737.4 (w)	-----		
875.1	871.9	871.0		vibrational LO mode of Nb-O in isolated groups such as NbO_6

The peak at 871 cm^{-1} is assigned to a vibrational LO mode of Nb–O in isolated groups such as NbO_6 , the bands 152 and 237 cm^{-1} belong to E(TO+LO) modes [10], while peaks at 279 , 336 and 629 cm^{-1} are known to belong to $A_1(\text{TO})$ modes, and they appear here at low temperatures only. Positions of $A_1(\text{TO})$ modes are in accordance with positions found by Ridah et al. [10], where they said that A_1 modes, for near stoichiometric LiNbO_3 , are lying around 252 , 275 , 332 and 632 cm^{-1} . The other authors gave positions of A_1 modes for near stoichiometric LiNbO_3 at 251 , 273 , 331 and 631 cm^{-1} [24], or 254 , 274 , 333 and 630 cm^{-1} [25], which are also in accordance with the obtained results.

Our experiment revealed that fundamental $A_1(\text{TO})$ bands of Nb^{5+} and Li^+ vibrations along the polar axis of the crystal within the oxygen octahedral (263 and 279 cm^{-1}) are well resolved at low temperature. Those lines shift to lower frequencies, and finally merge into a single broad maximum as temperature increases. This effect is explained as a result of inharmonic vibrations (quasi-soft-mode) and the two-phonon state. The presence of such an intense two-phonon scattering is a characteristic of the Raman spectrum in the oxide crystals and is induced by the large polarizability of the oxygen ion. Moreover, this scattering can be strongly affected by non-stoichiometric defects which break the Raman selection rules [22].

Raman intensity generally suffered abrupt changes for most of the bands in addition to frequencies shift. Moreover, the band at 332 cm^{-1} disappeared due to heating (at $+250\text{C}$) while the band at 262.5 cm^{-1} appeared strongly at high temperature, which means modification in the vibrational motions and crystal orientation of the NbO_6 octahedra due to enhancement of the weak Nb–O bond rocking against the O–Nb–O and Nb–O–Nb bending vibration at high temperature.

Also, new $A_1(\text{TO})$ bands appeared due to cooling, in addition to obvious splitting of the bands in the ranges 250 – 290 , 310 – 340 and 550 – 650 cm^{-1} (Fig. 2b–d), i.e. the 581 , 332 and 269 cm^{-1} vibrational modes split into two branches below $-100\text{ }^\circ\text{C}$. Since the original 581 cm^{-1} band corresponds to a totally symmetric NbO_6 stretching mode, this splitting can be interpreted as due to a distortion in the NbO_6 structure leading to two distinct sites for the NbO_6 unit below the transition region, where the presence of cluster-like regions of cations in LiNbO_3 crystals due to thermal treatment may disturb the normal vibrations of the ions. In fact, the mentioned above bands are correlated to bands splitting and shift due to thermal treatment where in general, heating caused almost all the peaks to shift towards lower frequency and vice versa due to the expected bonds softening and loosening due to heating, which affects the bonds force constant and frequency of vibration.

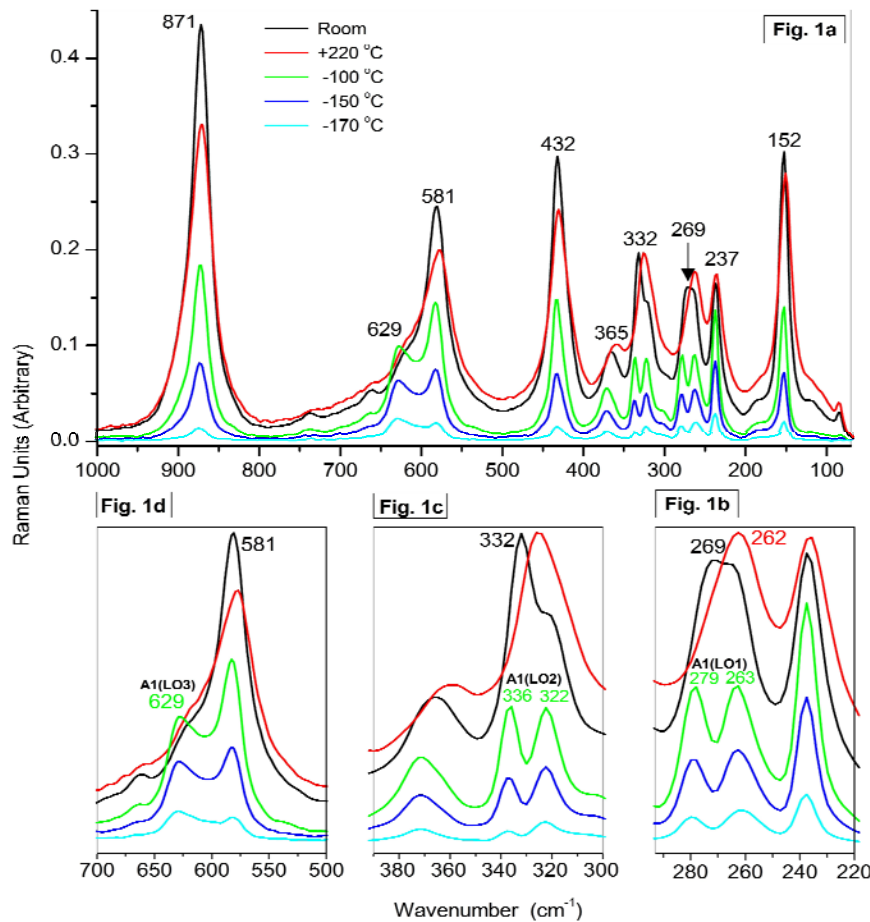


Figure (2): Raman scattering spectra of LiNbO₃

Band shape analysis was carried out and the temperature dependence of the frequency, intensity and band width were plotted for the bands: 152.9, 237, 271.5, 332, 365.7, 432.2, 581.2 and 871.9 cm⁻¹ as shown in Fig. (3), where the following remarks were observed:

1. The bands 152.9, 432.2 and 581.2 cm⁻¹ shifted to lower frequency with 2 rates (at +150 °C) due to heating, and to higher frequency with cooling down to -100 °C after which the frequency decreases again [Fig. (3a)]. Similar behavior was observed in their intensity [Fig. (3b)] and bandwidth temperature dependence [Fig. (3c)] where they decrease with cooling from -100°C, increase and then decrease with heating from +150°C. These phenomena can be related to the decrease of the dynamic disorder due to reorientational motions of NbO₆ octahedron taking place at low temperatures.

2. The rest of the bands (except the one at 871.9) showed systematic frequency shift with temperature with different rates of change, usually at -100°C and $+150^{\circ}\text{C}$. Same inversion points were clear in the intensity and bandwidth temperature dependence for all the bands as shown in Fig. (3).
3. The band 271.5 splitted into 2 bands at 261.5 and 271.5 cm^{-1} with cooling at -100°C and became one symmetric band centered at 262.5 cm^{-1} when $+225^{\circ}\text{C}$ was reached. As the sample was cooled down, splitting was recorded again with remarkable decrease in their intensities down to -196°C [Fig. (2b)]. Similar behavior was recorded for the doublet at 320-332 cm^{-1} [Fig. (2c)].
4. The complex contour at 581.7 cm^{-1} with a shoulder at 622.8 cm^{-1} showed an opposite behavior where its intensity decreased with both heating and cooling. Moreover, the shoulder became a separate band at -100°C , after which an abrupt decrease in the band intensities was observed with further cooling [Fig. (2d)].
- 5.

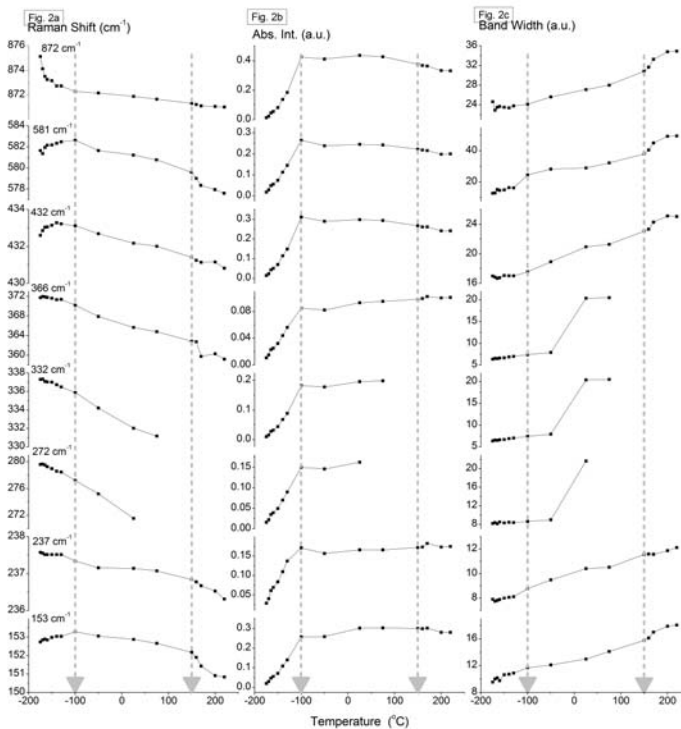


Figure (3): Experimental peak positions, symmetry and type of Raman-active modes in LiNbO_3 single crystal at different temperatures.

Raman shift is generally consistent with atomic displacements and structural modifications due to the lattice deformation caused by intrinsic defects and/or impurities and vacancies within the crystal. This phenomenon has been attributed to recovery process induced by relaxation. At this point of our discussion, it is consistent to say that changing temperature over a wide range induced modifications of the polarizability and a slight displacement of atoms which in turn modify their environment within the crystal lattice. The temperature dependence of the band parameters showed that an inversion point exists at $-100\text{ }^{\circ}\text{C}$ in the first cooling run at which the frequency shifts change their direction together with an abrupt decrease in the intensities of group of bands indicating that an abnormality in the structure of LiNbO_3 is taking place.

Line width (FWHM) and peak position of the stretching modes in NbO_6 octahedron versus temperature show a discontinuity near $-100\text{ }^{\circ}\text{C}$. These results indicate that a phase transition occurs at $-100\text{ }^{\circ}\text{C}$ on cooling and near $150\text{ }^{\circ}\text{C}$ on heating. Similar behavior was reported by Juanga et al [26] in pure NaNbO_3 and for the band 567 cm^{-1} in the case of LiNaNbO_3 where the wave number decreased with cooling while the line width increased at $-100\text{ }^{\circ}\text{C}$. This behavior is referred to a second order phase transition caused by the motion of cations against the NbO_6 octahedron which results in rapid shift to lower frequencies showing the so called soft mode. Band width of most of the bands decreased while cooling in the 1st run due to the decrease in the dynamic disorder caused by the reorientational motion of NbO_6 octahedron taking place during the phase transition, while disordering cause the bandwidth to increase with heating. 2nd run showed clearly that a hysteresis behavior exists, which mean that the structural changes occurring at $-100\text{ }^{\circ}\text{C}$ while cooling are kept to higher temperatures (-50 to $+80\text{ }^{\circ}\text{C}$) while heating as indicated by the abnormal temperature dependence of the intensity and frequency. Savatinova reported a similar behavior concerning a remarkable broadening of the vibrational bands leading to an overlap of the closely spaced bands in addition to the appearance of a new band at 70 cm^{-1} which was completely absent in the pure crystals of LiNbO_3 and LiTaO_3 crystals [4, 6].

The recorded behavior concerning the region of Nb-O stretching vibrations could be due to strong distortion of the niobium octahedral. On the other hand, the band characterizing the paraelectric phase of LiNbO_3 in the region 680 cm^{-1} showed a shift towards lower frequency due to heating from $-196\text{ }^{\circ}\text{C}$ to room temperature and an increase in the intensity associated with broadening up to room temperature. Finally, the obtained broadening and reduction in intensity could be referred to the existence of high degree of lattice disorder, together with two phases coexisting at the phase transition temperature, which might lead to breakdown in the selection rules leading to the observed experimental evidence indicating that all the vibrational bands of

LiNbO₃ including E and A modes can take part into scattering and forming broad spectral maxima.

4. Conclusions:

Low temperature Raman spectroscopic study performed on a Z-cut LiNbO₃ single crystal having Z(xy)Z configuration, indicated the detection of a newly reported second order phase transition occurring at -100°C on cooling and near +150°C on heating. The temperature dependence of the band parameters indicated the existence of a phase transition caused by the motion of cations against the NbO₆ octahedron which results in rapid shift to lower frequencies showing the so called "soft mode". The recorded behavior concerning the region of Nb-O stretching vibrations could be due to strong distortion of the niobium octahedral. Finally, the obtained broadening and reduction in intensity of some bands could be referred to the existence of high degree of lattice disorder, together with two phases coexisting at the phase transition temperature. This might lead to breakdown in the selection rules leading to the observed experimental evidence indicating that all the vibrational bands of LiNbO₃ can take part into scattering and forming broad spectral maxima.

References:

1. F. Caccavale, A. Morbiato, N. Natali, C. Sada and F. Segato, *J. Appl. Phys.* **87**, 1007 (2000),.
2. A.M. Glass, G.E. Peterson, T.J. Negran, in: A.M. Glass, A.H. Guenter (Eds.), *"Laser Induced Damage in Optical Materials"*, Spec. Publ. 372, US GPO, Washington, 15 (1972).
3. C.-H. Huang and L. McCaughan *IEEE J. Sel. Top. Quantum Electron.* **2**, 367 (1996).
4. I. Savova, I. Savatinova and E. Liarokapis, *Optical Materials*, **16** (3), 353 (2001).
5. I.P. Kaminow and W.D. Johnson, Jr., *Phys. Rev.* **160**, 519 (1967).
6. I. Savatinova, S. Tonchev and M. Kuneva, *Appl. Phys. A* **56**, 81 (1993).
7. B. Mihailova, N. Zotov, M. Marinov, J. Nikolov and L. Konstantinov, *J. Non-Cryst. Solids*, **168**, 265 (1994).
8. B. Mihailova, M. Marinov and L. Konstantinov, *J. Non-Cryst. Solids* **176**, 127 (1994).
9. Yu.K. Voron'ko, A.B. Kudryavtsev, V.V. Osiko, A. A. Sobol' and E.V. Sorokin, *Sov. Phys.-Solid State*, **29** (5), 771 (1987).
10. A. Ridah, M.D. Fontana and P. Bourson, *Phys. Rev. B*, **56**, 5967 (1997).
11. Y. Okamoto, Ping-chu Wang and J.F. Scott, *Phys. Rev. B*, **32**, 6787 (1985).
12. J.F. Scott, *Ferroelectric Rev.*, **1**, 111 (1998).

13. Y. Okamoto, P.-C. Wang, J.G. Scott, *Phys. Rev. B*, **32**, 6787 (1985).
14. E.B. De Aranjó, J.A.C. De Paiva, J.A. Freitas Jr., A.S.B. Sombra, *J. Phys. Chem. Solids*, **59**, 689 (1998).
15. S.C. Abrahams, J.M. Reddy and J.M. Bernstein, *J. Chem. Phys. Solids*, **27**, 997 (1966).
16. D.L. Rousseau, R.P. Bauman and S.P.S. Porto, *J. Raman Spectrosc.*, **10**, 253 (1981).
17. "Light scattering in solids", Int. conf. Paris 1971, Flammarion pp 247-252.
18. Shirane, R. Newnham, R. Pepinsky, *Phys. Rev.*, **96**, 581 (1954).
19. M.R. Beghoul, A. Boudrioua, R. Kremer, M.D. Fontana, B. Fougere, C. Darraud, J.C. Vareille and P. Moretti, *Optical Materials*, (2008)].
20. N.V. Sidorov, M.N. Palatnikov and Yu. A. Serebryakov, *Inorg. Mater.*, **33**, 496 (1997).
21. A.S. Barker Jr., R. Loudon, *Phys. Rev.*, **158**, 433 (1967).
22. A. Golubovi, R. Gaji, S. Nikoli, S. Duri and A. Valci, *J. Serb. Chem. Soc.*, **65**, 391 (2000).
23. W.D. Johnston Jr. and I.P. Kaminov, *Phys. Rev.*, **168**, 1045 (1968).
24. U.T. Schwartz and M. Maier, *Phys. Rev. B*, **55**, 11041 (1997).
25. V. Caciuc and A.V. Postnikov, *Phys. Rev. B*, **64**, 224303 (2001).
26. Y.D. Juanga, S.B. Daib, Y.C. Wangc, W.Y. Choub, J.S., Hwangb, M.L. Hud and W.S. Tse, *Solid State Communications*, **111**, 723 (1999)